Binding of Polyaminocarboxylate Chelators to the Active-Site Copper Inhibits the GSNO-Reductase Activity but Not the Superoxide Dismutase Activity of Cu,Zn-Superoxide Dismutase†

Mengwei Ye and Ann M. English*

Department of Chemistry and Biochemistry, Concordia University, 7141 Sherbrooke Street West, Montreal, Quebec H4B 1R6, Canada

Received May 30, 2006; Revised Manuscript Received August 28, 2006

ABSTRACT: In addition to its superoxide dismutase (SOD) activity, Cu,Zn-superoxide dismutase (CuZnSOD) catalyzes the reductive decomposition of *S*-nitroso-L-glutathione (GSNO) in the presence of thiols such as L-glutathione (GSH). The GSNO-reductase activity but not the superoxide dismutase (SOD) activity of CuZnSOD is inhibited by the commonly used polyaminocarboxylate metal ion chelators, EDTA and DTPA. The basis for this selective inhibition is systematically investigated here. Incubation with EDTA or DTPA caused a time-dependent decrease in the 680 nm d−d absorption of Cu^{II}ZnSOD but no loss in SOD activity or in the level of metal loading of the enzyme as determined by ICP-MS. The chelators also protected the SOD activity against inhibition by the arginine-specific reagent, phenylglyoxal. Measurements of both the time course of SNO absorption decay at 333 nm and oxymyoglobin scavenging of the NO that is released confirmed that the chelators inhibit CuZnSOD catalysis of GSNO reductive decomposition by GSH. The decreased GSNO-reductase activity is correlated with decreased rates of Cu^{II}ZnSOD reduction by GSH in the presence of the chelators as monitored spectrophotometrically at 680 nm. The aggregate data suggest binding of the chelators to CuZnSOD, which was detected by isothermal titration calorimetry (ITC). Dissociation constants of 0.08 ± 0.02 and 8.3 ± 0.2 μM were calculated from the ITC thermograms for the binding of a single EDTA and DTPA, respectively, to the CuZnSOD homodimer. No association was detected under the same conditions with the metal-free enzyme (EESOD). Thus, EDTA and DTPA must bind to the solvent-exposed active-site copper of one subunit without removing the metal. This induces a conformational change at the second active site that inhibits the GSNO-reductase but not the SOD activity of the enzyme.

Trace copper impurities found in aqueous buffers catalyze the reductive decomposition of *S*-nitrosothiols (RSNOs) (*1*−*6*). Recently, Dicks et al. demonstrated that generation of NO[1] from RSNOs was also catalyzed by peptide- and protein-bound copper (*7*), providing a mechanism for intracellular RSNO breakdown (*8*) since cells harbor no free copper (*9*). Jourd'heuil et al. (*10*) reported that Cu,Zn-superoxide dismutase (CuZnSOD) exhibits GSNO-reductase activity, yielding free NO in the presence of GSH:

$$Cu^{II}ZnSOD + GSH \rightleftharpoons Cu^{I}ZnSOD + GS^{\bullet} + H^{+} \quad (1)$$

$$Cu^{I}ZnSOD + GSNO + H^{+} \rightleftharpoons Cu^{II}ZnSOD + GSH + NO^{\bullet} \quad (2)$$

$$GS^{\bullet} + GS^{\bullet} \rightleftharpoons GSSG \quad (3)$$

Building on the work of Jourd'heuil et al. (*10*), we demonstrated that CuZnSOD is an efficient catalyst of the transfer of NO between *S*-nitrosoglutathione (GSNO) and Cysβ93 of oxyhemoglobin (oxyHb) (*11*) and Cys residues in calbindin D_{28K} (*12*) at physiological protein concentrations. We observed spectroscopically that both GSH and calbindin reduce Cu^{II}ZnSOD (*12*) and proposed a general mechanism for CuZnSOD-catalyzed S-nitrosation of protein-based thiols (P-SH) by GSNO (*12*):

$$Cu^{II}ZnSOD + P\text{-}SH \rightleftharpoons Cu^{I}ZnSOD + P\text{-}S^{\bullet} + H^{+} \quad (1')$$

$$Cu^{I}ZnSOD + GSNO + H^{+} \rightleftharpoons Cu^{II}ZnSOD + GSH + NO^{\bullet} \quad (2)$$

† This research was supported by grants from the Canadian Institutes for Health Research (CIHR) and the Natural Sciences and Engineering Research Council of Canada (NSERC) to A.M.E.

* To whom correspondence should be addressed: Department of Chemistry and Biochemistry, Concordia University, 7141 Sherbrooke St. W., Montreal, Quebec H4B 1R6, Canada. Phone: (514) 848-2424, ext. 3338. Fax: (514) 848-2868. E-mail: english@alcor.concordia.ca.

[1] Abbreviations: CuZnSOD, copper,zinc superoxide dismutase; cyt*c*, cytochrome *c*; DDC, diethyldithiocarbamic acid, sodium salt; DTPA, diethylenetriamine-*N*,*N*,*N*′,*N*″,*N*″-pentaacetic acid; EDTA, ethylenediamine-*N*,*N*,*N*′,*N*′-tetraacetic acid, disodium salt; EESOD, metal-free superoxide dismutase; GSH, glycine *N*-(*N*-L-γ-glutamyl-L-cysteinyl); GSNO, glycine *N*-(*N*-L-γ-glutamyl-*S*-nitroso-L-cysteinyl); GSSG, glycine *N*-(*N*-L-γ-glutamyl-L-cysteinyl) disulfide; ICP-MS, inductively coupled plasma mass spectrometry; ITC, isothermal titration calorimetry; Mb, myoglobin; $MbFe^{II}O_2$, oxymyoglobin; $MbFe^{III}$, metmyoglobin; neocuproine, 2,9-dimethyl-1,10-phenanthroline hydrochloride; NO, nitric oxide; PBS, phosphate-buffered saline [0.01 M sodium phosphate buffer (pH 7.4) with 0.0027 M KCl and 0.137 M NaCl]; P-SH, protein-base thiol.

10.1021/bi061077o CCC: $33.50
Published on Web 09/27/2006

$$NO^{\bullet} + P\text{-}S^{\bullet} \rightleftharpoons P\text{-}SNO \quad (4)$$

Unlike $GS^{\bullet}$ (eq 3) (*12*, *13*), dimerization of $P\text{-}S^{\bullet}$ is suppressed by steric bulk, allowing efficient protein S-nitrosation by the combination of $P\text{-}S^{\bullet}$ radicals with $NO^{\bullet}$ (eq 4) (*11*, *12*).

The SOD activity of CuZnSOD (eqs 5 and 6) also requires redox turnover of the active-site copper (*14*−*16*):

$$Cu^{II}ZnSOD + O_2^{\bullet-} \rightleftharpoons Cu^{I}ZnSOD + O_2 \quad (5)$$

$$Cu^{I}ZnSOD + O_2^{\bullet-} + 2H^{+} \rightleftharpoons Cu^{II}ZnSOD + H_2O_2 \quad (6)$$

Jourd'heuil et al. reported that 1 mM neocuproine, a Cu^{I}-specific chelator, had no effect on the SOD activity of CuZnSOD (eqs 5 and 6) but inhibited its GSNO-reductase activity (eqs 1 and 2). They also reported that the reductase activity was inhibited by the Cu^{II}-specific chelators, EDTA and DTPA, but no data or mechanism was provided (*10*). Consistent with the work of Jourd'heuil et al. (*10*), we found that the copper chelators additionally inhibited the NO-transferase activity of CuZnSOD (eqs 1′, 2, and 4) (*11*, *12*). Since EDTA and DTPA are used routinely in SOD assays (*14*, *17*, *18*) and in RSNO investigations (*13*, *19*, *20*), the purpose of this study is to explore the mechanism by which these anionic polyaminocarboxylate metal chelators selectively inhibit the GSNO-reductase activity of CuZnSOD.

The effects of EDTA and DTPA on (i) the d−d absorption of $Cu^{II}ZnSOD$, (ii) the reduction of $Cu^{II}ZnSOD$ by GSH, (iii) the metal-ion content of the enzyme, and its (iv) SOD and (v) GSNO-reductase activities were investigated. The ability of EDTA and DTPA to protect the SOD activity of CuZnSOD from phenylglyoxal-induced inactivation was also evaluated. Arg141 which is 5 Å from the catalytic copper (*21*) is critical for SOD activity (*21*−*30*), which is lost on modification of Arg141 with the arginine-specific reagent, phenylglyoxal (PGO) (*26*, *29*, *30*). Finally, isothermal titration calorimetry (ITC) was used to directly probe association of EDTA and DTPA with CuZnSOD and its metal-free form, EESOD (*14*, *31*−*33*).

Reaction 2 is likely a key common step in the S-nitrosation of protein thiols (P-SH) by GSNO, the most physiologically relevant NO donor identified to date (*34*−*38*). Thus, the GSNO-reductase activity of CuZnSOD may play a vital role in NO signaling in vivo, and the data presented here provide critical information about how the polyaminocarboxylate chelators modulate this activity in vitro and suggest possible mechanisms for its modulation in vivo.

MATERIALS AND METHODS

Materials

Bovine erythrocyte CuZnSOD (Roche Molecular Biochemicals) was used without further purification except where indicated. All reagents were analytical grade or better. GSNO [glycine *N*-(*N*-L-γ-glutamyl-*S*-nitroso-L-cysteinyl)] was obtained from Cayman. Horse heart myoglobin, horse heart cytochtome *c* (type III), xanthine, xanthine oxidase, PGO (phenylglyoxal hydrate), EDTA (ethylenediamine-*N*,*N*,*N*′,*N*′-tetraacetic acid, disodium salt), DDC (diethyl dithiocarbamate, sodium salt), neocuproine (2,9-dimethyl-1,10-phenanthroline hydrochloride), DTPA (diethylenetriamine-*N*,*N*,*N*′,*N*″,*N*″-pentaacetic acid), GSH (glutathione, reduced form), and GSSG (glutathione, oxidized form) were purchased from Sigma, and ultra-high purity concentrated HNO_3 was from EM Science. H_2O_2 (30%), 1000 ppm standard solutions (Cu and Zn) were purchased from ACP Chemicals Inc. Nanopure water (specific resistance of 18 MΩ-cm) obtained from a Millipore Simplicity water purification system was used to prepare all solutions. The sodium phosphate buffers used in the SOD activity assay and ITC measurements were treated with Chelex-100 resin (Bio-Rad) prior to being used to remove trace metal ions.

Methods

Effects of Chelators on CuZnSOD 680 nm Absorption. The concentration of CuZnSOD dissolved in 50 mM sodium phosphate buffer (pH 7.2) was determined spectrophotometrically ($\epsilon_{258} = 10\,300\ M^{-1}\ cm^{-1}$ per dimer) (*14*). Changes in the Cu^{II} d−d absorption of 200 μM enzyme at 680 nm ($\epsilon_{680} = 300\ M^{-1}\ cm^{-1}$ per dimer) (*14*) versus time were monitored at 37 °C in the presence of 5−10 mM EDTA, DTPA, GSH, and GSSG. All absorbance readings were carried out in 1 cm cells on an Agilent 8453 UV−visible diode array or a Beckman DU 650 spectrophotometer equipped with thermostated cell compartments.

CuZnSOD Modification by PGO. Modification of the arginine residues in CuZnSOD by PGO was carried out as described previously (*26*, *39*). Briefly, 105 μM CuZnSOD with and without 1 mM EDTA or DTPA or neocuproine was incubated with 4.2 mM PGO in 250 mM sodium bicarbonate (pH 8.0) with gentle shaking at room temperature for 6 h. Aliquots were removed from the reaction vials every hour, and the SOD activity was determined by the cytochrome *c* reduction assay as described below.

Xanthine Oxidase cytc^{III} Assay for SOD Activity. The SOD activity was determined from the competition between CuZnSOD and ferricytochrome *c* (cytc^{III}) for $O_2^{\bullet-}$, which decreases the rate of cytc^{III} reduction (*14*):

$$O_2^{\bullet-} \xrightarrow{cyt c^{III}} cyt c^{II} \quad (7)$$

$$O_2^{\bullet-} \xrightarrow{CuZnSOD} H_2O_2 + O_2 \quad (8)$$

Cytc^{III} reduction was initiated by adding xanthine oxidase to assay solutions containing 10 μM cytc^{III}, 50 μM xanthine, and 3.3 nM CuZnSOD in 50 mM sodium phosphate buffer (pH 7.8) at 25 °C. The xanthine oxidase concentration was adjusted to produce an initial ΔA_{550} of 0.025 ± 0.003 absorbance unit/min in a 1 cm path length cuvette, and A_{550} was read every 15 s over the course of 3 min to monitor cytc^{III} reduction. SOD activities were determined from the percent inhibition (*%I*, eq 9) of cytc^{III} reduction calculated from the initial slopes of A_{550} versus time plots generated in the absence ($Slope_{cytc^{III}}$) and presence of CuZnSOD ($Slope_s$). The relative SOD activities (eq 10) are the ratios of $\%I_c$ for the control (untreated CuZnSOD) and $\%I_s$ for the samples (CuZnSOD exposed to PGO or a chelator):

$$\%I = \frac{Slope_{cytc^{III}} - Slope_s}{Slope_{cytc^{III}}} \times 100 \quad (9)$$

$$\%\ \text{relative SOD activity} = \frac{\%I_s}{\%I_c} \times 100 \quad (10)$$

GSNO-Reductase Activity of CuZnSOD. Solutions containing GSNO, GSH, CuZnSOD, and EDTA or DTPA were incubated at 37 °C for 30 min to establish the extent of chelator inhibition of the GSNO-reductase activity of CuZnSOD (eqs 1−3). The decrease in the GSNO concentration was determined spectrophotometrically at the S−NO absorption band ($\epsilon_{333} = 0.767$ mM^{-1} cm^{-1}) (*40*).

Free NO is rapidly scavenged by oxymyoglobin (oxyMb, $MbFe^{II}O_2$), which is the basis of the oxyMb assay (*12*) used to monitor release of NO from GSNO:

$$NO + MbFe^{II}O_2 \rightleftharpoons NO_3^- + MbFe^{III} \qquad (11)$$

OxyMb was added to GSNO/GSH solutions with or without CuZnSOD and chelator, and the spectral changes upon conversion of oxyMb to metMb were monitored versus time.

ICP-MS Determination of the Metal-Ion Content of CuZnSOD. The levels of copper and zinc loading of CuZnSOD following incubation with the chelators were determined by inductively coupled plasma mass spectrometry (ICP-MS). CuZnSOD was incubated with 5 mM EDTA, DTPA, or DDC at 37 °C for 30 min. Since DDC is known to remove copper at neutral pH (*41*), the DDC/CuZnSOD incubation was included with the controls (CuZnSOD without chelators and the chelators alone). Acetone (1.0 mL) was added to 100 μL aliquots of the incubations, and after they stood at −20 °C for 30 min, the precipitated protein was washed twice with cold acetone. The SOD activity was measured before and after acetone treatment to ensure complete enzyme precipitation, and after centrifugation at 12000*g* for 7 min, the supernatants were removed with micropipettes and the precipitates were dried on a Speed Vac (SC 110, Savant). The residues were transferred quantitatively to 10 mL beakers, digested at 90 °C with 1 mL of concentrated HNO_3 and 100 μL of 30% H_2O_2, and diluted to a final volume of 10.0 mL with deionized water. Samples were introduced into the torch of a PE Sciex Elan 6000 ICP-MS device via a cross-flow nebulizer/Scott-type spray chamber system. The RF power was 1000 W and the rate of argon flow 0.85 L/min, which gave the best sensitivity as determined by the recommended optimization procedure. The optimum lens voltage was determined by maximizing the rhodium sensitivity, and data were acquired in the pulse-count mode (*42*).

Preparation of EESOD. The metal-free enzyme was prepared by 24 h dialysis at 4 °C of CuZnSOD against 50 mM sodium acetate buffer (pH 3.8) containing 10 mM EDTA (*14*). EDTA-free EESOD was obtained as described previously (*31*) via a 24 h dialysis against three changes of 50 mM sodium acetate buffer (pH 5) and a 24 h dialysis against two changes of 0.1 M $NaClO_4$ in 50 mM sodium phosphate buffer (pH 7.4) followed by a 24 h dialysis against three changes of 50 mM sodium phosphate buffer (pH 7.4).

ITC Analysis of CuZnSOD−Chelator and EESOD−Chelator Association. Protein samples were prepared by overnight dialysis against Chelex-treated 50 mM sodium phosphate buffer (pH 7.4). EDTA (a 50.1 mM standard solution, Aldrich) and DTPA (>99% pure powder, Sigma) were added to the dialysis buffer, and the pH was adjusted to 7.4 using ultrapure NaOH (Fluka) to ensure minimal background from buffer mismatch. A known concentration of protein determined spectrophotometrically [$\epsilon_{258} = 10\,300$ M^{-1} cm^{-1} (CuZnSOD dimer) and $\epsilon_{258} = 2920$ M^{-1} cm^{-1} (EESOD dimer) (*14*, *31*)] was added to the cell of a VP-ITC microcalorimeter (MicroCal) following degassing of the protein and chelator solutions using the ThermoVac (MicroCal). The chelator was injected with 300 rpm stirring at discrete intervals into the cell, and the heat per injection was measured. The observed heats were corrected for the heat of dilution of the chelator by performing control titrations in the absence of protein, and the resulting thermograms were analyzed using Origin for ITC supplied by MicroCal.

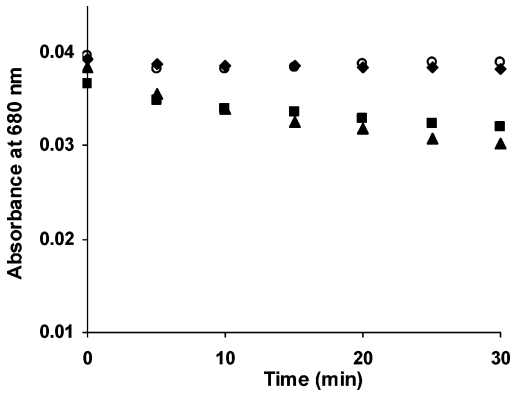

FIGURE 1: Cu^{II} d−d absorption at 680 nm vs time in incubations of 200 μM CuZnSOD with EDTA, DTPA, or GSSG: CuZnSOD only (◆) or CuZnSOD with 10 mM DTPA (■), 10 mM EDTA (▲), and 5 mM GSSG (○). Samples were in 50 mM sodium phosphate buffer (pH 7.2), and the absorbance at 680 nm was recorded at 5 min intervals after addition of EDTA, DTPA, or GSSG to Cu^{II}ZnSOD at 37 °C.

Table 1: Cu and Zn Concentrations of CuZnSOD Samples Determined by ICP-MS

sample[a]	[Cu] ± SD (μM)[b]	[Zn] ± SD (μM)[b]
0.6 μM CuZnSOD	1.41 ± 0.326	1.28 ± 0.233
50 μM EDTA	0.19 ± 0.036	0.42 ± 0.052
50 μM DTPA	0.24 ± 0.036	0.06 ± 0.044
50 μM DDC	0.21 ± 0.005	0.35 ± 0.043
0.6 μM CuZnSOD and EDTA	1.40 ± 0.085	1.14 ± 0.198
0.6 μM CuZnSOD and DTPA	1.42 ± 0.230	1.11 ± 0.087
0.6 μM CuZnSOD and DDC	0.33 ± 0.027	0.71 ± 0.154

[a] CuZnSOD (60 μM) in PBS (pH 7.4) was incubated with 5 mM EDTA, DTPA, or DDC at 37 °C for 30 min and precipitated with acetone. The precipitates were digested with acid and diluted 10^3-fold for the ICP-MS analysis (see the text). [b] Values are the averages of three separate trials.

RESULTS

Effects of Chelators on CuZnSOD 680 nm Absorption. Cu^{II}ZnSOD exhibits a weak Cu^{II} d−d absorption band at 680 nm ($\epsilon = 300$ M^{-1} cm^{-1} per dimer) (*14*). This band is sensitive to changes in Cu^{II} ligation and geometry and is lost upon reduction of the enzyme to Cu^{I}ZnSOD (*14*, *43*, *44*). As we reported previously (*12*), a 30 min incubation at 37 °C of Cu^{II}ZnSOD alone or with GSSG resulted in the negligible loss of 680 nm absorbance, but addition of DTPA and EDTA decreased the absorbance at 680 nm by ∼20% (Figure 1). This loss could be caused by copper reduction or removal and/or by conformational changes induced by the presence of the chelators.

Effects of Chelators on the Metal-Ion Content of CuZnSOD. The ICP-MS results in Table 1 reveal that within experimental error there is no loss of copper or zinc from CuZnSOD following preincubation with EDTA or DTPA.

Consistent with the spectrophotometric data (not shown), DDC removed 77% of the Cu from CuZnSOD as well as 44% of the Zn (Table 1). Unlike EDTA, DDC is known to remove copper from the enzyme at neutral pH (*41*, *45*).

Effects of Chelators on Cu^{II}ZnSOD Reduction. Figure 2A shows the decrease in the magnitude of the 680 nm band over 30 min after addition of 5 mM GSH to Cu^{II}ZnSOD, which can be readily reduced ($E°_{Cu^{II/I}} = 0.28-0.42$ V) (*44*, *46*). Addition of 3.3 mM EDTA or DTPA significantly inhibited reduction of the active-site Cu^{II} (Figure 2B), indicating that the chelators interfere with the transfer of electrons from GSH to the copper possibly by interacting with CuZnSOD close to its active-site channel.

Effects of Chelators and GSH on SOD Activity. Using the xanthine oxidase−cytc^{III} assay (eqs 7 and 8) (*14*, *18*, *47*), SOD activity was found to be linear with CuZnSOD concentration up to 6 nM enzyme (data not shown) as reported previously (*48*). To prevent interference from trace metal contaminants, 0.1−1 mM EDTA or DTPA is routinely added to SOD activity assays (*14*, *18*, *49*). As shown in Table 2, negligible SOD activity changes were observed in the presence of 0.1−2 mM EDTA or DTPA as reported for the pyrogallol autoxidation assay (*18*).

Figure 3 shows that CuZnSOD preincubation at pH 7.2 and 37 °C for 0−60 min with 2 mM EDTA, DTPA, or GSSG or 5 mM GSH had no effect on its SOD activity. Since thiols interfere with the xanthine oxidase−cytc^{III} assay by reducing cytc^{III} (*48*), 5 mM GSH was added to the assay solution just prior to the measurement being taken. The activity of the control (CuZnSOD that was not preincubated with GSH) was also measured in the presence of thiol. The results reveal that although GSH reduces Cu^{II}ZnSOD (Figure 2A), this does not interfere with its SOD activity (Figure 3). Consistent with previous reports (*41*, *45*), a 20 min CuZnSOD preincubation with DDC at pH 7.2 resulted in a >90% SOD activity loss (data not shown), which is attributed to removal of Cu from the enzyme (Table 1).

Effects of Chelators on PGO Inactivation of SOD Activity. Aliquots removed from the PGO incubations were diluted ~10^3-fold into the SOD assay solution. After a 6 h preincubation with a 40-fold molar excess of PGO, CuZnSOD exhibited ~25% SOD activity (Figure 4), consistent with reports that PGO modification of Arg141 resulted in the loss of 80−97% of the SOD activity (*22*, *25*, *26*). Addition of EDTA or DTPA to the incubations increased the SOD activity remaining after 6 h to ~43% (Figure 4), suggesting that these chelators had a protective effect on Arg141. In contrast, the uncharged copper chelator, neocuproine, offered CuZnSOD no protection against PGO inactivation (Figure 4).

Effects of Chelators and GSH on the GSNO-Reductase Activity of CuZnSOD. In the presence of 30 μM CuZnSOD and 5 mM GSH, ~170 μM GSNO decomposed in 30 min at 37 °C (data not shown). Addition of 2 mM DTPA or EDTA decreased the level of GSNO decomposition to 47 or 59%, respectively (Figure 5), consistent with the chelators' inhibition of reduction of Cu^{II}ZnSOD by GSH (Figure 2B). The data in Figure 5 also show that the chelators inhibit GSNO decomposition in the absence of the enzyme, indicating that trace copper impurities contribute to GSNO breakdown. However, this is only 32% of the GSNO breakdown observed in the presence of CuZnSOD (Figure 5).

Table 2: SOD Activity of CuZnSOD in the Presence of EDTA and DTPA[a]

chelator[b]	% inhibition ± SD[c]	% relative SOD activity[d]
none	49.01 ± 0.39	100
0.1 mM EDTA	49.02 ± 1.45	100
2.0 mM EDTA	49.17 ± 0.94	100
0.1 mM DTPA	48.25 ± 0.58	98.4
2.0 mM DTPA	48.59 ± 0.45	99.1

[a] Assay solutions contained 10 μM cytc^{III}, 3.3 nM CuZnSOD, and 50 μM xanthine with or without chelator in Chelex-100-treated 50 mM sodium phosphate buffer (pH 7.8), 25 °C. The assay was triggered by the addition of ~3.5 units/L xanthine oxidase. [b] Concentration of the chelator in the assay solution. [c] CuZnSOD inhibition of reduction of cytc^{III} by $O_2^{\bullet-}$ as calculated using eq 9. Values given are the averages of three measurements. [d] The SOD activity of 3.3 nM CuZnSOD in the absence of chelator was taken to be 100%.

Release of NO from GSNO (eq 2) was confirmed using oxyMb as a scavenger (eq 11). In the presence of GSNO alone, ~5 μM oxyMb was converted to metMb over 20 min (Figure 6A), consistent with the decomposition of ~5 μM GSNO over 30 min in buffer only (data not shown). Addition of CuZnSOD and GSH to the oxyMb/GSNO incubation resulted in the conversion of the limiting (25 μM) oxyMb present to metMb in <4 min (Figure 6B), and release of NO was retarded on addition of DTPA or EDTA since oxyMb peaks are still clearly visible in the spectra after 20 min (Figure 6C,D).

Thermodynamic Parameters for Association of EDTA and DTPA with CuZnSOD. ITC was employed in examining the association of EDTA and DTPA with CuZnSOD and

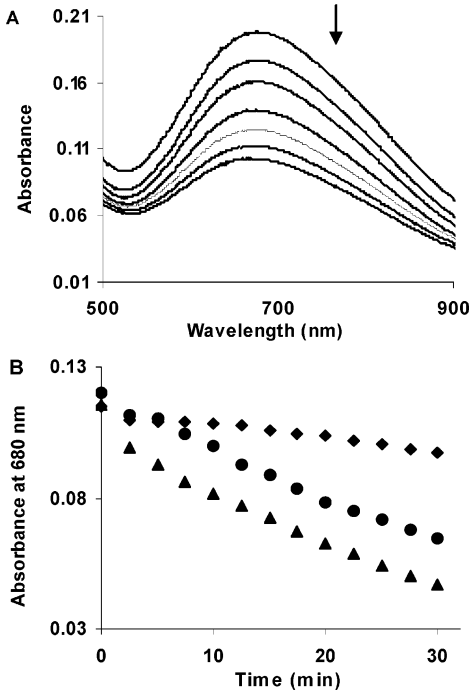

FIGURE 2: Cu^{II} d−d absorption at 680 nm vs time of CuZnSOD/GSH incubations with and without EDTA or DTPA. (A) Spectrum of 690 μM CuZnSOD with 5 mM GSH at 0, 2.5, 5, 10, 15, 20, and 30 min. (B) Data points are the absorbance at 680 nm vs time of samples containing 400 μM CuZnSOD with 3.3 mM GSH (▲), 3.3 mM EDTA (●), or 3.3 mM DTPA (◆). Absorbance values of samples in 50 mM sodium phosphate buffer (pH 7.2) were recorded in a 1 cm cuvette at 37 °C immediately after addition of GSH, DTPA, or EDTA to CuZnSOD ($t = 0$ min) and at 2.5 min intervals over the course of 30 min.

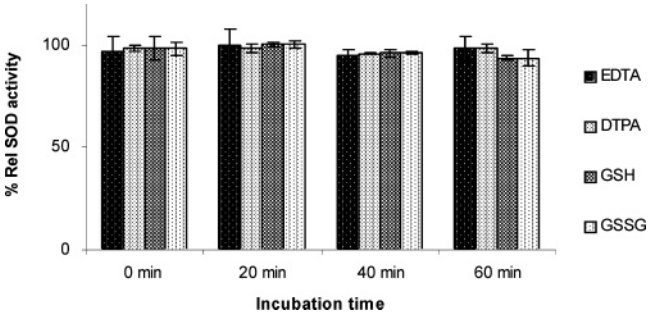

FIGURE 3: Effects of preincubation with chelators, GSSG or GSH, on SOD activity of CuZnSOD. CuZnSOD (20 μM) was preincubated with 2 mM EDTA, 2 mM DTPA, 2 mM GSSG or 5 mM GSH in 50 mM sodium phosphate buffer (pH 7.2) at 37 °C for 60 min. Aliquots were removed every 20 min and assayed for SOD activity. Assay solutions contained 10 μM cytc^{III}, 50 μM xanthine, and 3.3 nM CuZnSOD in 50 mM sodium phosphate buffer and 0.1 mM EDTA (pH 7.8). Where indicated, 2 mM chelator or 2 mM GSSG was also present in the assay solution. To trigger the assay, ~3.5 units/L xanthine oxidase was added (as well as 5 mM GSH to the assays containing this reagent). The relative SOD activity of untreated CuZnSOD was taken to be 100%.

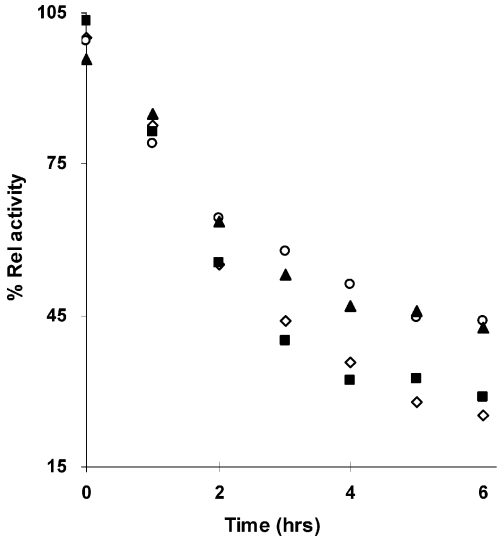

FIGURE 4: Effects of preincubation with PGO without or with EDTA or DTPA on SOD activity of CuZnSOD: CuZnSOD with PGO only (◇) and in the presence of 1 mM EDTA (▲), 1 mM DTPA (○), or 1 mM neocuproine (■). In the experiment, 105 μM CuZnSOD was incubated with 4.2 mM PGO in 250 mM Na_2CO_3 (pH 8.0) with or without 1 mM chelators with gentle shaking at room temperature for 6 h. Aliquots were removed and diluted 70-fold, and 10 μL was added to 3 mL of 50 mM sodium phosphate and 0.1 mM EDTA (pH 7.8) and assayed for SOD activity as described in Materials and Methods. The relative SOD activity of CuZnSOD from <1 min incubations was taken to be 100%.

EESOD. The heat change upon ligand binding to a protein is given by the relationship $\Delta H_b = \Delta H_{ITC} - \Delta H_{blank}$, where ΔH_{ITC} is the apparent heat of binding measured by ITC and ΔH_{blank} corrects for dilution of the ligand into the buffer only. The raw data obtained in the titration of CuZnSOD with the chelators as ligands (Figure 7, top panels) reveal that DTPA binding is an endothermic process while EDTA binding is largely exothermic. The thermograms corresponding to integrated heat versus chelator/CuZnSOD dimer molar ratio are displayed in the bottom panels. The Origin software provides three curve fitting models involving one or two sets of binding sites and sequential binding sites (*50*). Best fits were

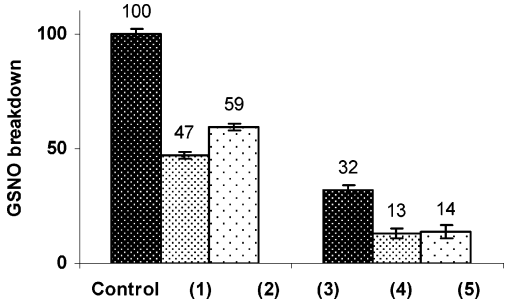

FIGURE 5: Effects of EDTA and DTPA on the GSNO-reductase activity of CuZnSOD with GSH as a donor substrate: (Control) GSNO/GSH/CuZnSOD, (1) GSNO/GSH/CuZnSOD/DTPA, (2) GSNO/GSH/CuZnSOD/EDTA, (3) GSNO/GSH, (4) GSNO/GSH/DTPA, and (5) GSNO/GSH/EDTA incubations. In the experiment, solutions containing 470 μM GSNO, 5 mM GSH, 30 μM CuZnSOD, 2 mM DTPA, and 2 mM EDTA where indicated were incubated in 50 mM sodium phosphate buffer (pH 7.2) at 37 °C for 30 min. The amount of GSNO remaining was determined spectrophotometrically ($\epsilon_{333} = 0.76$ mM^{-1} cm^{-1}), and the decomposition of 170 μM GSNO in the control was normalized to 100%. Each bar represents the mean ± the standard deviation of triplicate determinations.

obtained using one set of binding sites for DTPA and two sets of sites for EDTA (Figure 7, bottom panels).

The apparent number of chelator binding sites (n) per CuZnSOD dimer and the thermodynamic parameters, including the dissociation constant (K_d), the enthalpy of binding (ΔH), and the entropy of binding (ΔS), are listed in Table 3. One EDTA molecule per CuZnSOD dimer binds to the high-affinity site with a K_d of ~80 nM. Thus, a single EDTA molecule interacts with both monomers, or EDTA binding to one monomer inhibits binding of a second EDTA molecule to the dimer. The stoichiometry of the EDTA low-affinity site ($K_d \sim 4$ μM) is 0.2−0.4 chelator molecule per dimer, which suggests that binding of EDTA to the high-affinity site inhibits binding of a second EDTA molecule. On the basis of the K_d values (Table 3), the affinity of DTPA for the CuZnSOD dimer is 2 orders of magnitude lower than that for EDTA at 25 °C. Furthermore, the negative ΔH_b and positive ΔS_b values reveal that binding of EDTA to CuZnSOD is both enthalpically and entropically favorable, whereas both ΔH_b and ΔS_b values are positive for DTPA, indicating that DTPA binding is entropically driven. Significantly, binding to the low-affinity EDTA site exhibits binding parameters similar to those obtained for DTPA, especially at 37 °C. Also, since the 25 and 37 °C enthalpy and entropy values vary, the chelator−CuZnSOD complexes may undergo temperature-dependent rearrangement.

Association of the chelators with metal-free EESOD was also examined. Contrary to expectation, the same heat changes were recorded on titration of the buffer (ΔH_{blank}) (data not shown) and EESOD with both EDTA and DTPA (ΔH_{ITC}) (Figure 8). Thus, the EESOD thermograms show no heat changes revealing that the metals promote the association of the chelators with CuZnSOD.

DISCUSSION

The ITC data summarized in Table 3 reveal that the CuZnSOD homodimer binds a single polyaminocarboxylate chelator. K_d values of 0.08 and 8.3 μM, at 25 °C, were obtained for association of EDTA and DTPA, respectively,

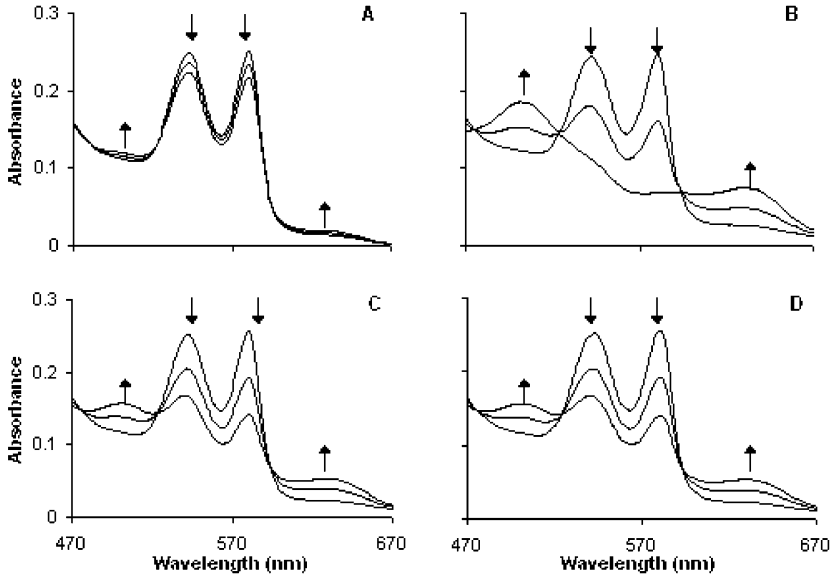

FIGURE 6: OxyMb assay of effects of metal chelators on the release of NO from GSNO: (A) oxyMb/GSNO, (B) oxyMb/GSNO/GSH/CuZnSOD, (C) oxyMb/GSNO/GSH/CuZnSOD/EDTA, and (D) oxyMb/GSNO/GSH/CuZnSOD/DTPA incubations. In the experiment, 25 μM oxyMb and 145 M GSNO were incubated with 1 mM GSH, 20 μM CuZnSOD, and 1 mM chelator (where indicated) in 50 mM sodium phosphate buffer (pH 7.2) at 37 °C for 20 min. Spectra in panel A were recorded in a 1 cm cuvette at 0, 12, and 20 min, in panel B at 0, 2, and 4 min, and in panels C and D at 0, 12, and 20 min. The down arrows at 542 and 580 nm indicate oxyMb decay, and the up arrows at 502 and 632 nm indicate metMb growth.

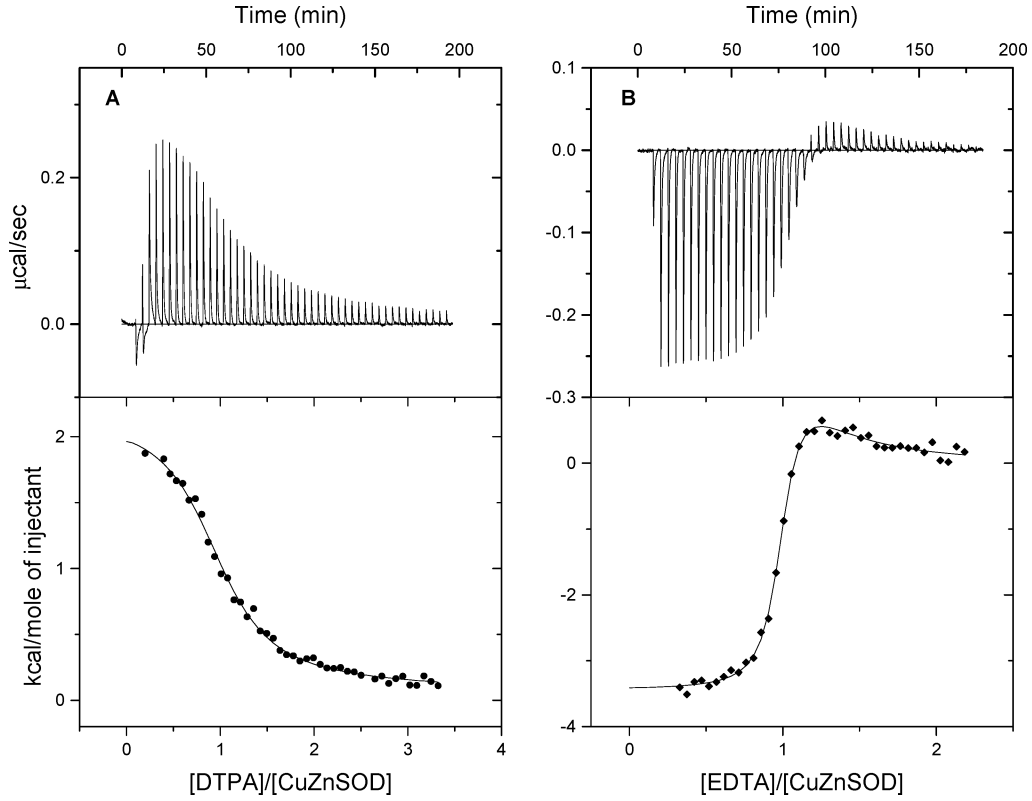

FIGURE 7: ITC analysis of binding of EDTA and DTPA to CuZnSOD. (A) Aliquots (5 μL) of 806 μM DTPA were injected into the 1.5 mL ITC cell containing CuZnSOD at an initial concentration of 41.0 μM at 37 °C. (B) Aliquots (5 μL) of 501 μM EDTA were injected into the 1.5 mL ITC cell containing CuZnSOD at an initial concentration of 36.1 μM at 25 °C. Both protein and chelators were in 50 mM phosphate buffer (pH 7.4). Top panels show the raw data for 45−48 injections of chelator into the CuZnSOD solution at 4 min intervals. The data points in the bottom panels are the integrated heats of binding (ΔH_b) after subtraction of the blank (ΔH_{blank}). The solid lines correspond to the best fits of the data to (A) one set of binding sites and (B) two sets of binding sites using Origin software.

with the enzyme, and a second low-affinity EDTA site was also detected but with a low binding stoichometry (Table 3). Since it was previously reported that Arg141 is a phosphate binding site in CuZnSOD (*25*) and EESOD binds EDTA (*31*), we presumed that the chelator binding site included Arg141 and possibly Lys120 and/or Lys134 (Figure 9A). However, no evidence for association of the chelators with metal-free EESOD was obtained by ITC (Figure 8), indicating that the active-site copper is necessary for the high-affinity binding observed here.

Table 3: Thermodynamic Parameters from the Titration of CuZnSOD with EDTA and DTPA[a]

chelator[b] (*T*)	*n*[c]	K_d (μM)	ΔH_b (kcal/mol)	ΔS_b (cal K^{-1} mol^{-1})
EDTA (25 °C)	1.09 ± 0.16	0.08 ± 0.02	−3.42 ± 0.02	21.05 ± 0.7
EDTA (37 °C)	0.83 ± 0.16	0.03 ± 0.02	−2.59 ± 0.41	24.29 ± 4.9
EDTA (25 °C)	0.23 ± 0.01	4.25 ± 11.1	3.65 ± 0.07	36.39 ± 2.1
EDTA (37 °C)	0.38 ± 0.03	3.25 ± 3.12	2.21 ± 0.28	32.24 ± 1.8
DTPA (25 °C)	0.97 ± 0.04	8.26 ± 0.20	1.19 ± 0.24	27.23 ± 0.8
DTPA (37 °C)	1.04 ± 0.02	7.58 ± 0.99	2.43 ± 0.20	31.25 ± 0.4

[a] Data were fit to two-binding-site (EDTA) and one-binding-site (DTPA) models using Origin software. The binding parameters given are the average of three measurements. [b] The experimental conditions are given in the legend of Figure 7. The ITC experiments were performed at the indicated temperatures (*T*). [c] The stoichiometry of binding is the chelator/CuZnSOD dimer molar ratio.

The X-ray structure shows that active-site cavity of bovine CuZnSOD is ~15 Å deep and 12 Å wide near the protein surface and narrows to ~3 Å at the catalytic copper, which has a solvent-exposed surface area of ~5 $Å^2$. The copper is coordinated by His44, His46, His61, His118, and a weakly bound water molecule which occupies the axial position of a distorted square pyramid and is directed toward the cavity opening. Strong ligands such as CN^- and N_3^- bind to Cu^{II}-ZnSOD and cause a weakening of the Cu−His46 bond (*51*). The zinc, which is completely buried in the protein, is bridged to the copper by the imidazolate side chain of His61. Since the only access to the copper is from the active-site cavity, the chelators must enter the channel. This interaction would be promoted by the positive residues lining the channel such as Arg141, Lys120, and Lys134 (Figure 9A). In fact, it has been suggested that phosphate bridges Arg141 and cobalt in the CoZnSOD metalloderivative, leading to cleavage of the imidazolate bridge and movement of the tetrahedral cobalt toward the cavity (*52*). A similar situation can be envisaged whereby the copper moves toward an oxygen donor atom of the chelator but remains bound to the polypeptide, which has a high affinity for the metal (K_d = 6 fM) (*9*). Consistent with this proposal, the Cu^{II}ZnSOD−chelator complexes are $>10^{11}$-fold less stable than the $Cu(EDTA)^{2-}$ and $Cu(DTPA)^{3-}$ complexes with log K_a values of 8.8 and 21.1, respectively (*53*). The ICP-MS analysis (Table 1) confirmed that EDTA or DTPA does not sequester any metal from CuZnSOD at pH 7.4. In contrast, incubation with DDC, which is known to remove copper from the enzyme at neutral pH (*41*, *54*), led to significant demetallation (Table 1), and EESOD was formed in EDTA incubations at pH 3.8 (*14*, *31*, *32*) with loss of SOD activity (data not shown).

A network of well-ordered water molecules is found in the active-site cavity of CuZnSOD. This network extends from the bottom of the cavity in two directions and connects the copper-bound water to the solvent. The large favorable entropies for chelator binding (21−36 eu, Table 3) are consistent with release of water from the cavity to the bulk solvent as well as dissociation of the aquo and histidyl ligands from the copper. The latter bond cleavages are expected to be enthalpically unfavorable and would contribute to the low binding enthalpies observed for the chelators. In particular, the positive binding enthalpy for DTPA suggests that there is negative compensation between bond making and breaking in the CuZnSOD−DTPA complex. Ionization of the chelators, which are hexaprotic (EDTA) and octaprotic (DTPA) acids, may also contribute to the observed heats of binding.

The data in Figures 1, 2, and 4 provide additional support for the binding of the chelators in the active-site channel. The loss of the 680 nm d−d absorption (Figure 1) may be due to direct Cu^{II}−EDTA and Cu^{II}−DTPA binding as well as to additional interaction with Arg141 since modification of this residue is known to alter the d−d absorption (*26*). GSH is a poorer reductant of Cu^{II}ZnSOD in the presence of the chelators (Figure 2B), which could reflect decreased GSH accessibility to the copper in the enzyme−chelator complexes. Less SOD activity was lost in CuZnSOD/PGO incubations containing EDTA or DTPA (Figure 4), suggesting that the chelators decreased the access of PGO to Arg141 which is ~5 Å from the copper. On the basis of NMR data (*55*), binding of formate via H-bonding of its oxygens to the Nϵ and NH_2 atoms of the Arg141 side chain was proposed. The formate carboxylate carbon, also ~5 Å from the copper, did not displace the coordinated water (*55*). However, the additional carboxylate groups in the polyaminocarboxylate chelators would allow them to bind the active-site copper as well as Arg141, which would explain their affinity for the protein being 10^4−10^6-fold higher [K_d = 0.08−8 μM (Table 3)] than that for formate (K_d = 0.24 M).

Relevant to the 2/1 Cu^{II}/chelator stoichiometry observed here (Table 3), it was found that both $Fe(CN)_6^{3-}$ and $IrCl_6^{2-}$ bound preferentially to a single CuZnSOD subunit, rendering one of the Cu^{II} atoms nontitratable (*46*). The iridium complex was used to form a heavy atom derivative of CuZnSOD, and the major $IrCl_6^{2-}$ binding site involves Arg141 (*56*). Thus, binding of a large anion in the active-site cavity of one subunit appears to induce a conformational change at the other active site, although the copper atoms are 34 Å apart (*56*).

Coordination of EDTA with the active-site copper was visualized by manually docking EDTA into the active-site channel with PyMol (Figure 9B). Docking the chelator into the static enzyme molecule demonstrates that, contrary to expectation, one of EDTA's carboxylate groups can coordinate to the active-site copper without reorganization of groups in the active-site cavity. Furthermore, the concentration of positive electrostatic potential (blue) around the cavity (Figure 9) should promote binding of anionic ligands in the cavity. Nonetheless, copper binding has also been observed for uncharged ligands, which underscores the accessibility and reactivity of the metal. For example, addition of singly charged DDC and neutral neocuproine to Cu^{II}ZnSOD gave rise to new visible absorption bands between 450 and 460 nm, but after dilution of the enzyme into the assay buffer, no loss of SOD activity was observed (*10*, *45*).

Why Do the Chelators Selectively Inhibit the GSNO-Reductase Activity of CuZnSOD? The inhibitory effect of DTPA and EDTA on the GSNO-reductase activity of CuZnSOD (eqs 1 and 2) is demonstrated in Figures 5 and 6. Since Cu^{I}-catalyzed RSNO breakdown is rapid (*5*), the rate-limiting step in GSNO turnover by the CuZnSOD/GSH mixture is assumed to be formation of the cuprous enzyme (eq 1). As shown here, the chelators retard Cu^{II}ZnSOD reduction by GSH (Figure 2B). Additionally, the GSSG oxidation product, known to chelate Cu^{II} and inhibit free copper-catalyzed GSNO decomposition (*3*, *6*), likely inhibits reduction of Cu^{II}ZnSOD by GSH since the enzyme is not fully reduced even in the presence of a large excess of this thiol (*12*). Also, Jourd'heuil et al. (*10*) observed 90% decom-

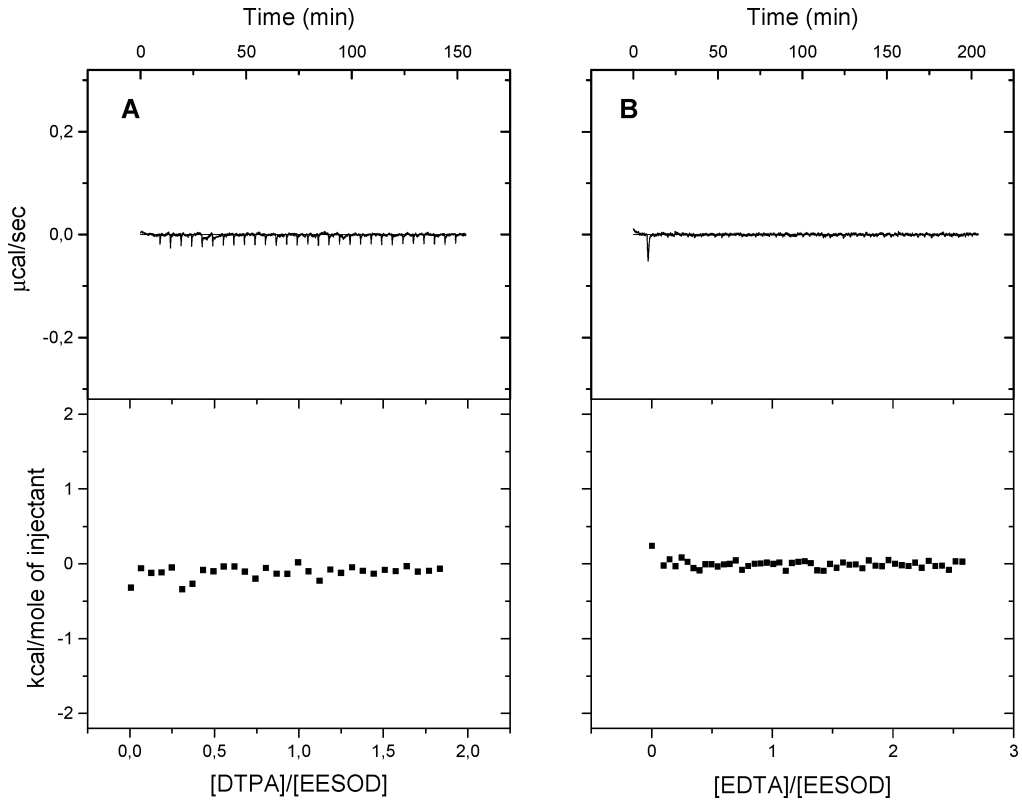

FIGURE 8: ITC analysis of binding of EDTA and DTPA to EESOD. Aliquots (5 μL) of 1 mM DTPA (A) or 806 μM EDTA (B) were injected into the 1.5 mL ITC cell containing EESOD at an initial concentration of 55.4 μM at 37 °C. Both protein and chelators were in 50 mM phosphate buffer (pH 7.4). Top panels show the raw data for 30−50 injections of chelator into the EESOD solution at 4 min intervals. The data points in the bottom panels show the integrated heats.

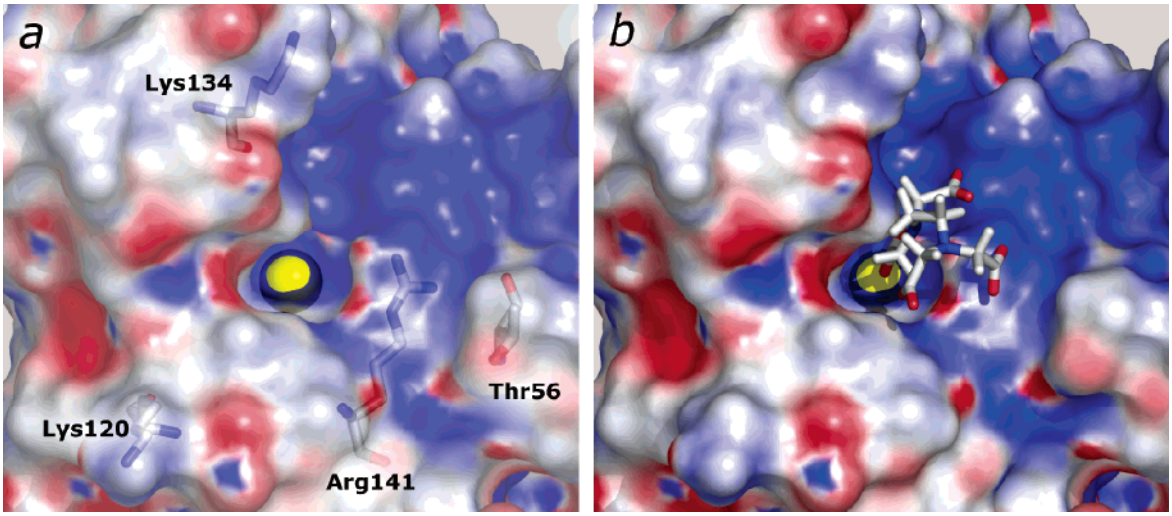

FIGURE 9: Docking of EDTA into the active-site channel of bovine CuZnSOD. (A) Molecular surface and electrostatic potential map (blue, positive; red, negative) of the active-site channel of CuZnSOD. Thr56 and Glu131 form the opening of the active-site cavity. An electrostatic loop consisting of the positively charged side chains of Arg141, Lys120, and Lys134 guides the anionic superoxide substrate to the copper center. Arg141 and Thr135 act as a "bottleneck" for the active site, limiting the access of bulky anions to the copper shown as a yellow sphere at the bottom of the active-site channel (*63*). (B) Docking of the EDTA molecule into the active-site channel demonstrates that a carboxylic group of EDTA can access the active-site copper. The electrostatic potential surface of CuZnSOD was obtained using the reported crystal structure (*64*), which was preprocessed with PDB2PQR (*65*), and the electrostatic potential was calculated with the APBS package (*66*) and visualized with PyMOL (*67*).

position of 10 μM GSNO by CuZnSOD in the presence of 50 μM GSH, whereas we observed only 36% decomposition of 470 μM GSNO in the presence of 5 mM GSH (see the legend of Figure 5), which is consistent with product inhibition by the GSSG generated during GSNO decomposition (eq 3). However, as we reported previously (*12*), addition of 5 mM GSSG did not alter the 680 nm absorption of CuZnSOD (Figure 1) or its SOD activity (Figure 3).

The members of an electrostatic loop, the positively charged side chains of Arg141, Lys120, and Lys134 (Figure 9A), are 5, 12, and 13 Å, respectively, from the copper (*21*, *25*). These residues promote access of superoxide, small

anionic inhibitors such as cyanide, and water to the copper (*23*, *24*, *28*, *29*, *57*). The reported bimolecular rate constant for reduction of Cu^{II}ZnSOD by $O_2^{\bullet-}$, which involves direct binding of $O_2^{\bullet-}$ to Cu^{II}, is $\sim 2 \times 10^9$ M^{-1} s^{-1} at 25 °C (*14*, *16*, *58*). Binding of superoxide to the enzyme is the rate-limiting step in SOD catalysis (*59*, *60*), and saturation is not observed in assays carried out at low superoxide concentrations such as those used here. Since binding of neither EDTA nor DTPA alters the SOD activity (Table 2), the chelators must not alter the overall rate of reduction of Cu^{II} by $O_2^{\bullet-}$. CuZnSOD binds one chelator per homodimer (Table 3), so it is possible that only one copper is active in $O_2^{\bullet-}$ turnover in the CuZnSOD−chelator complexes. Thus, binding of the chelator to one copper must increase the SOD activity and decrease the GSNO-reductase activity at the second copper. The latter observation is in fact consistent with the negative cooperativity in the association of the chelators, as well as $Fe(CN)_6^{3-}$ and $IrCl_6^{2-}$, with CuZnSOD. Since the homodimer does not bind two large ligands, it is not surprising that large substrates such as GSH and GSNO have decreased access to the second copper in the CuZnSOD−chelator complexes. Alternatively, CuZnSOD may exhibit half-site reactivity in both its free and chelator-bound forms, with both forms possessing the same SOD activity but with only the free form possessing GSNO-reductase activity. Half-site reactivity has been demonstrated for enzymes composed of identical subunits such as the tyrosyl-tRNA synthase homodimer (*61*).

CONCLUSIONS

CuZnSOD, abundant in red blood cells and many other cell types, likely mediates NO metabolism by "moonlighting" as a GSNO reductase. Given its high affinity for a single EDTA or DTPA ligand, negatively charged metabolites such as 2,3-diphosphoglycerate found in red blood cells (*62*) may bind to CuZnSOD in vivo and modulate NO signaling by altering its GSNO-reductase (eqs 1 and 2) or NO-transferase (eqs 1′, 2, and 4) activities. The negative cooperativity in binding large anions exhibited by CuZnSOD may serve to control GSNO turnover and/or prevent nonproductive GSH turnover in vivo. However, since the chelators do not inhibit SOD activity, O_2^- turnover at the single free copper in the CuZnSOD−chelator complexes must be double that in the free enzyme unless CuZnSOD exhibits half-site reactivity. Irrespective of such mechanistic details, it is essential to consider the effects of polyaminocarboxylate chelators on the GSNO-reductase activity of CuZnSOD in studies of GSNO and NO biochemistry.

ACKNOWLEDGMENT

We thank Professor Eric Salin and Megan Marshall from the Department of Chemistry, McGill University (Montreal, PQ), for help with the ICP-MS measurements and Dr. Qadir Timerghazin for preparing Figure 9.

REFERENCES

1. Gorren, A. C., Schrammel, A., Schmidt, K., and Mayer, B. (1996) Decomposition of S-nitrosoglutathione in the presence of copper ions and glutathione, *Arch. Biochem. Biophys. 330*, 219−228.
2. Singh, R. J., Hogg, N., Joseph, J., and Kalyanaraman, B. (1996) Mechanism of nitric oxide release from S-nitrosothiols, *J. Biol. Chem. 271*, 18596−18603.
3. Noble, D. R. S., Helen, R., Williams, D., and Lyn, H. (1999) Nitric oxide release from S-nitrosoglutathione (GSNO), *Chem. Commun.*, 2317−2318.
4. Noble, D. R., and Williams, D. L. (2000) Structure-reactivity studies of the Cu^{2+}-catalyzed decomposition of four S-nitrosothiols based around the S-nitrosocysteine/S-nitrosoglutathione structures, *Nitric Oxide 4*, 392−398.
5. Burg, A., Cohen, H., and Meyerstein, D. (2000) The reaction mechanism of nitrosothiols with copper(I), *J. Biol. Inorg. Chem. 5*, 213−217.
6. Stubauer, G., Giuffre, A., and Sarti, P. (1999) Mechanism of S-nitrosothiol formation and degradation mediated by copper ions, *J. Biol. Chem. 274*, 28128−28133.
7. Dicks, A. P., and Williams, D. L. (1996) Generation of nitric oxide from S-nitrosothiols using protein-bound Cu^{2+} sources, *Chem. Biol. 3*, 655−659.
8. Johnson, M. A., Macdonald, T. L., Mannick, J. B., Conaway, M. R., and Gaston, B. (2001) Accelerated S-nitrosothiol breakdown by amyotrophic lateral sclerosis mutant copper, zinc-superoxide dismutase, *J. Biol. Chem. 276*, 39872−39878.
9. Rae, T. D., Schmidt, P. J., Pufahl, R. A., Culotta, V. C., and O'Halloran, T. V. (1999) Undetectable intracellular free copper: The requirement of a copper chaperone for superoxide dismutase, *Science 284*, 805−808.
10. Jourd'heuil, D., Laroux, F. S., Miles, A. M., Wink, D. A., and Grisham, M. B. (1999) Effect of superoxide dismutase on the stability of S-nitrosothiols, *Arch. Biochem. Biophys. 361*, 323−330.
11. Romeo, A. A., Capobianco, J. A., and English, A. M. (2003) Superoxide dismutase targets NO from GSNO to Cysb93 of oxyhemoglobin in concentrated but not dilute solutions of the protein, *J. Am. Chem. Soc. 125*, 14370−14378.
12. Tao, L., and English, A. M. (2003) Mechanism of S-nitrosation of recombinant human brain calbindin D_{28K}, *Biochemistry 42*, 3326−3334.
13. Romeo, A. A., Capobianco, J. A., and English, A. M. (2002) Heme nitrosylation of deoxyhemoglobin by S-nitrosoglutathione requires copper, *J. Biol. Chem. 277*, 24135−24141.
14. McCord, J. M., and Fridovich, I. (1969) Superoxide dismutase. An enzymic function for erythrocuprein (hemocuprein), *J. Biol. Chem. 244*, 6049−6055.
15. Fridovich, I. (1983) Superoxide radical: An endogenous toxicant, *Annu. Rev. Pharmacol. Toxicol. 23*, 239−257.
16. Fridovich, I. (1986) Superoxide dismutases, *Adv. Enzymol. Relat. Areas Mol. Biol. 58*, 61−97.
17. Winterbourn, C. C., Peskin, A. V., and Parsons-Mair, H. N. (2002) Thiol oxidase activity of copper, zinc superoxide dismutase, *J. Biol. Chem. 277*, 1906−1911.
18. Marklund, S., and Marklund, G. (1974) Involvement of the superoxide anion radical in the autoxidation of pyrogallol and a convenient assay for superoxide dismutase, *Eur. J. Biochem. 47*, 469−474.
19. Bryan, N. S., Rassaf, T., Maloney, R. E., Rodriguez, C. M., Saijo, F., Rodriguez, J. R., and Feelisch, M. (2004) Cellular targets and mechanisms of nitros(yl)ation: An insight into their nature and kinetics in vivo, *Proc. Natl. Acad. Sci. U.S.A. 101*, 4308−4313.
20. Jia, L., Bonaventura, C., Bonaventura, J., and Stamler, J. S. (1996) S-Nitrosohaemoglobin: A dynamic activity of blood involved in vascular control, *Nature 380*, 221−226.
21. Tainer, J. A., Getzoff, E. D., Beem, K. M., Richardson, J. S., and Richardson, D. C. (1982) Determination and analysis of the 2 Å-structure of copper, zinc superoxide dismutase, *J. Mol. Biol. 160*, 181−217.
22. Beyer, W. F., Jr., Fridovich, I., Mullenbach, G. T., and Hallewell, R. (1987) Examination of the role of arginine-143 in the human copper and zinc superoxide dismutase by site-specific mutagenesis, *J. Biol. Chem. 262*, 11182−11187.
23. Fisher, C. L., Cabelli, D. E., Tainer, J. A., Hallewell, R. A., and Getzoff, E. D. (1994) The role of arginine 143 in the electrostatics and mechanism of Cu,Zn superoxide dismutase: Computational and experimental evaluation by mutational analysis, *Proteins 19*, 24−34.
24. Bertini, I. A., Lepori, C., Luchinat, P., and Turano, P. (1991) Role of Arg-143 in human Cu_2Zn_2SOD studied through anion binding, *Inorg. Chem. 30*, 3363−3364.
25. Mota de Freitas, D., and Valentine, J. S. (1984) Phosphate is an inhibitor of copper-zinc superoxide dismutase, *Biochemistry 23*, 2079−2082.

26. Malinowski, D. P., and Fridovich, I. (1979) Chemical modification of arginine at the active site of the bovine erythrocyte superoxide dismutase, *Biochemistry 18*, 5909−5917.
27. Tainer, J. A., Getzoff, E. D., Richardson, J. S., and Richardson, D. C. (1983) Structure and mechanism of copper, zinc superoxide dismutase, *Nature 306*, 284−287.
28. Getzoff, E. D., Tainer, J. A., Weiner, P. K., Kollman, P. A., Richardson, J. S., and Richardson, D. C. (1983) Electrostatic recognition between superoxide and copper, zinc superoxide dismutase, *Nature 306*, 287−290.
29. Cudd, A., and Fridovich, I. (1982) Electrostatic interactions in the reaction mechanism of bovine erythrocyte superoxide dismutase, *J. Biol. Chem. 257*, 11443−11447.
30. Bermingham-McDonogh, O., Mota de Freitas, D., Kumamoto, A., Saunders, J. E., Blech, D. M., Borders, C. L., Jr., and Valentine, J. S. (1982) Reduced anion-binding affinity of Cu,Zn superoxide dismutases chemically modified at arginine, *Biochem. Biophys. Res. Commun. 108*, 1376−1382.
31. Fee, J. A. (1973) Studies on the reconstitution of bovine erythrocyte superoxide dismutase. IV. Preparation and some properties of the enzyme in which Co^{II} is substituted for Zn^{II}, *J. Biol. Chem. 248*, 4229−4234.
32. Carrico, R. J., and Deutsch, H. F. (1970) The presence of zinc in human cytocuprein and some properties of the apoprotein, *J. Biol. Chem. 245*, 723−727.
33. Weser, U., Barth, G., Djerassi, C., Hartmann, H. J., Krauss, P., Voelcker, G., Voelter, W., and Voetsch, W. (1972) A study on purified apo-erythrocuprein, *Biochim. Biophys. Acta 278*, 28−44.
34. Arnelle, D. R., and Stamler, J. S. (1995) NO^+, NO, and NO^- donation by S-nitrosothiols: Implications for regulation of physiological functions by S-nitrosylation and acceleration of disulfide formation, *Arch. Biochem. Biophys. 318*, 279−285.
35. Konorev, E. A., Tarpey, M. M., Joseph, J., Baker, J. E., and Kalyanaraman, B. (1995) S-Nitrosoglutathione improves functional recovery in the isolated rat heart after cardioplegic ischemic arrest-evidence for a cardioprotective effect of nitric oxide, *J. Pharmacol. Exp. Ther. 274*, 200−206.
36. Rauhala, P., Lin, A. M., and Chiueh, C. C. (1998) Neuroprotection by S-nitrosoglutathione of brain dopamine neurons from oxidative stress, *FASEB J. 12*, 165−173.
37. Radomski, M. W., Rees, D. D., Dutra, A., and Moncada, S. (1992) S-Nitroso-glutathione inhibits platelet activation in vitro and in vivo, *Br. J. Pharmacol. 107*, 745−749.
38. Padgett, C. M., and Whorton, A. R. (1998) Cellular responses to nitric oxide: Role of protein S-thiolation/dethiolation, *Arch. Biochem. Biophys. 358*, 232−242.
39. Takahashi, K. (1977) The reactions of phenylglyoxal and related reagents with amino acids, *J. Biochem. 81*, 395−402.
40. Hogg, N., Singh, R. J., and Kalyanaraman, B. (1996) The role of glutathione in the transport and catabolism of nitric oxide, *FEBS Lett. 382*, 223−228.
41. Cocco, D., Calabrese, L., Rigo, A., Argese, E., and Rotilio, G. (1981) Re-examination of the reaction of diethyldithiocarbamate with the copper of superoxide dismutase, *J. Biol. Chem. 256*, 8983−8986.
42. Abbyad, P., Tromp, J., Lam, J., and Salin, E. (2001) Optimization of the technique of standard additions for inductively coupled plasma mass spectrometry, *J. Anal. At. Spectrom. 16*, 464−469.
43. Fee, J. A., and Gaber, B. P. (1972) Anion binding to bovine erythrocyte superoxide dismutase. Evidence for multiple binding sites with qualitatively different properties, *J. Biol. Chem. 247*, 60−65.
44. Fee, J. A., and DiCorleto, P. E. (1973) Observations on the oxidation-reduction properties of bovine erythrocyte superoxide dismutase, *Biochemistry 12*, 4893−4899.
45. Misra, H. P. (1979) Reaction of copper-zinc superoxide dismutase with diethyldithiocarbamate, *J. Biol. Chem. 254*, 11623−11628.
46. Lawrence, G. D., and Sawyer, D. T. (1979) Potentiometric titrations and oxidation-reduction potentials of manganese and copper-zinc superoxide dismutases, *Biochemistry 18*, 3045−3050.
47. McCord, J. M., and Fridovich, I. (1968) The reduction of cytochrome c by milk xanthine oxidase, *J. Biol. Chem. 243*, 5753−5760.
48. Flohe, L., and Otting, F. (1984) Superoxide dismutase assays, *Methods Enzymol. 105*, 93−104.
49. Butler, J., Koppenol, W. H., and Margoliash, E. (1982) Kinetics and mechanism of the reduction of ferricytochrome c by the superoxide anion, *J. Biol. Chem. 257*, 10747−10750.
50. MicroCal, Inc. (1998) *ITC Data Analysis in Origin Tutorial Guide*, version 5.0.9.
51. Carugo, K. D., Battistoni, A., Carri, M. T., Polticelli, F., Desideri, A., Rotilio, G., Coda, A., and Bolognesi, M. (1994) Crystal structure of the cyanide-inhibited *Xenopus laevis* Cu,Zn superoxide dismutase at 98 K, *FEBS Lett. 349*, 93−98.
52. Banci, L., Bertini, I., Luchinat, C., Monnanni, R., and Scozzafava, A. (1987) Characterization of the cobalt(II)-substituted superoxide dismutase-phosphate systems, *Inorg. Chem. 26*, 153−156.
53. Chaberek, S., Frost, A. E., Doran, M. A., and Bicknelll, N. J. (1959) Interaction of some divalent metal ions with diethylene-triaminepentaacetic acid, *J. Inorg. Nucl. Chem. 11*, 184−196.
54. Cocco, D., Calabrese, L., Rigo, A., Marmocchi, F., and Rotilio, G. (1981) Preparation of selectively metal-free and metal-substituted derivatives by reaction of Cu−Zn superoxide dismutase with diethyldithiocarbamate, *Biochem. J. 199*, 675−680.
55. Sette, M., Paci, M., Desideri, A., and Rotilio, G. (1992) Formate as an NMR probe of anion binding to Cu,Zn and Cu,Co bovine erythrocyte superoxide dismutases, *Biochemistry 31*, 12410−12415.
56. Richardson, J., Thomas, K. A., Rubin, B. H., and Richardson, D. C. (1975) Crystal structure of bovine Cu,Zn superoxide dismutase at 3 Å resolution: Chain tracing and metal ligands, *Proc. Natl. Acad. Sci. U.S.A. 72*, 1349−1353.
57. Polticelli, F., Battistoni, A., O'Neill, P., Rotilio, G., and Desideri, A. (1998) Role of the electrostatic loop charged residues in Cu,-Zn superoxide dismutase, *Protein Sci. 7*, 2354−2358.
58. Pantoliano, M. W., Valentine, J. S., Burger, A. R., and Lippard, S. J. (1982) A pH-dependent superoxide dismutase activity for zinc-free bovine erythrocuprein. Reexamination of the role of zinc in the holoprotein, *J. Inorg. Biochem. 17*, 325−341.
59. Klug, D., Rabani, J., and Fridovich, I. (1972) A direct demonstration of the catalytic action of superoxide dismutase through the use of pulse radiolysis, *J. Biol. Chem. 247*, 4839−4842.
60. Takahashi, M., and Asada, K. (1982) A flash-photometric method for determination of reactivity of superoxide: Application to superoxide dismutase assay, *J. Biochem. 91*, 889−896.
61. Fersht, A. R., Mulvey, R. S., and Koch, G. L. (1975) Ligand binding and enzymic catalysis coupled through subunits in tyrosyl-tRNA synthetase, *Biochemistry 14*, 13−18.
62. Wiback, S. J., and Palsson, B. O. (2002) Extreme pathway analysis of human red blood cell metabolism, *Biophys. J. 83*, 808−818.
63. Getzoff, E. D., Hallewell, R. A., and Tainer, J. A. (1986) *Protein Engineering: Applications in science, medicine and industry*, Academic Press, Orlando, FL.
64. Rypniewski, W. R., Mangani, S., Bruni, B., Orioli, P. L., Casati, M., and Wilson, K. S. (1995) Crystal Structure of Reduced Bovine Erythrocyte Superoxide Dismutase at 1.9 Å Resolution, *J. Mol. Biol. 251*, 282−296.
65. Dolinsky, T. J., Nielsen, J. E., McCammon, J. A., and Baker, N. A. (2004) PDB2PQR: An automated pipeline for the setup of Poisson-Boltzmann electrostatics calculations, *Nucleic Acids Res. 32*, W665−W667.
66. Baker, N. A., Sept, D., Joseph, S., Holst, M. J., and McCammon, J. A. (2001) Electrostatics of nanosystems: Application to microtubules and the ribosome, *Proc. Natl. Acad. Sci. U.S.A. 98*, 10037−10041.
67. DeLano, W. L. (2002) *The PyMOL Molecular Graphics System*, DeLano Scientific, San Carlos, CA.

BI061077O